Thrombosis Research 236 (2024) 201–208

Contents lists available at ScienceDirect

Thrombosis Research

journal homepage: www.elsevier.com/locate/thromres

Impact of allele-selective silencing of von Willebrand factor in mice based on a single nucleotide allelic difference in von Willebrand factor

Yvonne K. Jongejan [a], Noa A. Linthorst [a], Elisa Schrader Echeverri [b], Sebastiaan N.J. Laan [a], Richard J. Dirven [a], James E. Dahlman [b], Bart J.M. van Vlijmen [a], Cécile V. Denis [c], Jeroen C. J. Eikenboom [a,*]

[a] Department of Internal Medicine, Division of Thrombosis and Hemostasis, Einthoven Laboratory for Vascular and Regenerative Medicine, Leiden University Medical Center, Leiden, the Netherlands
[b] Wallace H. Coulter Department of Biomedical Engineering, Georgia Institute of Technology and Emory University School of Medicine, Atlanta, GA, United States
[c] Laboratory for Hemostasis, Inflammation and Thrombosis, Unité Mixed de Recherche S1176, Institut National de la Santé et de la Recherche Médicale, Université Paris-Saclay, Le Kremlin-Bicêtre, France

ARTICLE INFO

Keywords:
Von Willebrand factor
siRNA
Allele-selective silencing
Murine models
Thrombosis
Bleeding

ABSTRACT

Introduction: Von Willebrand factor (VWF) plays a pathophysiological role in hemostatic disorders. Partial inhibition of the *VWF* gene through small interfering RNA (siRNA)-mediated allele-selective silencing could be a promising therapeutic strategy. For von Willebrand disease, allele-selectively inhibiting dominant-negative *VWF*-alleles might ameliorate the phenotype. For thrombotic disorders, partial VWF reduction can lower thrombotic risk, while avoiding bleeding. Previously, we demonstrated the feasibility of *Vwf*-silencing in homozygous C57BL/6J (B6) or 129S1/SvImJ (129S) mice. The present study investigated allele-selective *Vwf*-silencing in a complex heterozygous setting of crossed B6 and 129S mice and its subsequent hemostatic impact.
Materials and methods: Heterozygous B6.129S mice were treated with siRNAs targeting *Vwf* expressed from either B6- (si*Vwf.B6*) or 129S-alleles (si*Vwf.129S*). Plasma VWF and lung *Vwf* mRNA were determined. si*Vwf.B6*-treated B6.129S mice were subjected to ferric chloride-induced mesenteric vessel thrombosis and tail-bleeding.
Results: In B6.129S mice, si*Vwf.B6* reduced *Vwf* mRNA of the targeted B6-allele by 72% vs. only 12% of the non-targeted 129S-allele (41% total mRNA reduction), lowering plasma VWF by 46%. Oppositely, si*Vwf.129S* reduced *Vwf* mRNA by 45%, now selectively inhibiting the 129S-allele over the B6-allele (58% vs. 9%), decreasing plasma VWF by 43%. The allele-selective VWF reduction by si*Vwf.B6* coincided with decreased thrombus formation in mesenteric arterioles, without prolonging tail-bleeding times.
Conclusions: This study demonstrates the feasibility of allele-selective *Vwf*-silencing in a heterozygous setting, achieving a controlled close to 50% reduction of plasma VWF. The observed thromboprotection and absence of prolonged bleeding times underline the potential of allele-selective *Vwf*-silencing as a therapeutic strategy in hemostatic disorders.

1. Introduction

The multimeric plasma glycoprotein von Willebrand factor (VWF) plays a pivotal role in the primary hemostasis [1]. It also functions in the secondary hemostasis as the carrier protein for coagulation factor VIII (FVIII) as it forms a noncovalent complex with FVIII [2,3]. Deficient or low VWF activity levels in plasma could lead to the bleeding disorder von Willebrand disease (VWD) [4]. VWD is the most common inherited bleeding disorder. In roughly 70 % of the VWD patients, a disease-causing mutation in the *VWF* gene can be identified, most of which have a dominant-negative effect [4,5]. In contrast, elevated plasma VWF levels are associated with an increased risk of developing arterial and venous thrombosis [6,7]. Although direct evidence for a causal relationship of high VWF and thrombosis is lacking, a causal relationship is indirectly supported by the observation that low VWF is associated with reduced cardiovascular disease and mortality, and even more so by the

* Corresponding author at: Department of Internal Medicine, Division of Thrombosis and Hemostasis, Einthoven Laboratory for Vascular and Regenerative Medicine, Leiden University Medical Center, P.O. Box 9600, 2300 RC Leiden, the Netherlands.
E-mail address: h.c.j.eikenboom@lumc.nl (J.C.J. Eikenboom).

https://doi.org/10.1016/j.thromres.2024.03.002
Received 12 December 2023; Received in revised form 6 February 2024; Accepted 4 March 2024
Available online 5 March 2024

protective effect of VWD for developing thrombotic events, such as coronary artery disease and ischemic stroke [8,9]. Additionally, ultra-large VWF multimers as a result of reduced activity of the VWF cleaving protease ADAMTS13 (a disintegrin and metalloprotease with thrombospondin type 1 repeats, member 13), lead to thrombotic thrombocytopenic purpura [10].

As VWF plays a central pathophysiological role in these different hemostatic disorders, targeting VWF itself is an interesting therapeutic approach. For VWD, current treatment strategies focus on increasing circulating plasma VWF via either infusion of VWF concentrate or stimulating endogenous release of endothelial VWF [11,12]. However, neither of these inhibits the formation of mutant VWF, which in itself could result in negative effects. Treatment strategies addressing the thrombotic properties of VWF have focused on blocking its hemostatic function, with the unwanted effect of an increasing risk of bleeding [13,14]. An alternative strategy to substituting VWF or targeting the release or function of VWF could be the reduction of VWF production via inhibition of the translation of *VWF* mRNA. In the case of VWD, inhibition of production should solely focus on the mutant dominant-negative *VWF*-allele, leaving the other normal *VWF*-allele unimpaired. This will result in an improvement of the activity and function of the remaining normal VWF. In the context of thrombotic disorders, the goal would also be to inhibit the production of one *VWF*-allele only to partially lower VWF production while avoiding too low plasma levels that might coincide with a bleeding risk.

Allele-selective silencing of the *VWF* gene using small interfering RNAs (siRNAs) could be suitable for achieving such a partial reduction in VWF production. This strategy could be applied to only inhibit the mutated *VWF*-allele to ameliorate the VWD phenotype. In thrombotic disorders, allele-selective silencing of *VWF* would allow for a maximal reduction of VWF production by 50%, averting an increased bleeding risk. Therapeutic allele-selective siRNAs have the ability to silence one allele based on a single nucleotide allelic difference, as has been shown for other autosomal dominant diseases [15,16]. As VWD can be caused by hundreds of different mutations in the *VWF* gene [5], it is not feasible to develop siRNAs targeting the specific unique mutation. In the case of elevated levels of VWF associated with thrombosis, there are actually no mutations present that could be targeted [8,17]. Therefore, a universal alternative approach could be targeting of common genetic variations within the *VWF* gene, such as the well-documented single nucleotide polymorphisms (SNPs) [18].

Previously, we have demonstrated the feasibility of designing siRNAs to silence murine *Vwf* from the commonly used mouse inbred strains, C57BL/6J (B6) or 129S1/SvImJ (129S), differing at the target site by a single nucleotide. These two mouse inbred strains were chosen based on the presence of differences in the sequence of their *Vwf* genes and comparable plasma VWF levels. siRNAs targeted towards *Vwf* of B6 or 129S mice were tested *in vivo* and proved to be strain-selective [19]. However, these experiments were only performed in a homozygous setting, in either the B6 or 129S mouse [19]. In a more complex heterozygous setting of crosses of B6 and 129S that includes the presence of competing targeted and non-targeted *Vwf*-alleles, allele-selective silencing of *Vwf* is expected to be more challenging, which may impact efficacy as well as the selectivity of the siRNAs.

In the present study, we crossed B6 and 129S mice and tested whether allele-selective silencing is also achievable in these heterozygous mice. After confirming allele-selectivity of the siRNAs on both mRNA and plasma levels, the hemostatic impact of such allele-selective silencing was assessed by subjecting mice to thrombotic and bleeding challenges.

2. Methods

2.1. Animals

C57BL/6J (B6) and 129S1/SvImJ (129S) mouse strains were chosen based on the presence of 11 nucleotides differing between their *Vwf* genes and their comparable plasma VWF levels [19]. B6 male and female mice (mouse strain #000664, The Jackson Laboratory, Bar Harbor, ME, USA) were obtained from Charles River, France. Female 129S mice (#002448) were obtained directly from The Jackson Laboratory, Bar Harbor, ME, USA. At the inhouse animal facilities B6 males and 129S females were intercrossed to produce hybrid F1 offspring B6.129S. For assessment of allele-selectivity of the siRNAs and in the tail-bleeding experiments, 5–8 weeks old B6.129S and B6 male and female mice were used. Post-weaning, 3–4 weeks old B6.129S and B6 male and female mice were used for the ferric chloride ($FeCl_3$)-induced thrombosis model. B6.129S2-*Vwf*^{tm1Wgr}/J mice (*Vwf*$^{-/-}$, backcrossed on a B6 background; #003795, The Jackson Laboratory) were used as a reference control in the tail-bleeding experiments. Mice were housed in conventional cages with a 12:12 h light-dark cycle with ad libitum access to food and water. Experimental setup was in accordance with the Institute for Laboratory Animal Research Guide for the Care and Use of Laboratory Animals and had received approval from the Ethical Review Boards for Animal Experimentation of the Leiden University Medical Center, Leiden, The Netherlands and INSERM (APAFIS #38228-202208021331789 v2), Le Kremlin-Bicêtre, France for the studies performed at their respective institutes. Sample sizes were determined using non-parametric power calculations with G*Power version 3.1.9.4 [20]. Animals were randomized using RandoMice software [21]. In all experiments, the primary researcher was blinded to the treatment order and animal treatment history at sacrifice until data analysis.

2.2. siRNA formulation, delivery and in vivo administration

siRNAs designed to target the *Vwf*-allele of either the B6 (si*Vwf.B6*) or 129S (si*Vwf.129S*) mouse strain, a non-selective si*Vwf* and corresponding scrambled controls (si*Control*, si*Control.B6*, si*Control.129S*) were designed and tested previously on *in vitro* and *in vivo* effectivity and strain-selectivity [19]. siRNA design (Table 1) and manufacturing was done by Axolabs (Kulmbach, Germany). For endothelial delivery, siRNAs were encapsulated in 7C1 lipid nanoparticles as previously described at the Atlanta facilities [22,23]. siRNA-encapsulated nanoparticles were cool packed and shipped from Atlanta, USA to Leiden, The Netherlands or Le Kremlin-Bicêtre, Paris, France (in case of $FeCl_3$-induced thrombosis studies, see below) and stored at 4°C. The nanoparticles were used within four weeks after formulation to ensure stability. Mice were given a single intravenous tail vein injection with siRNA-encapsulated nanoparticles at a previously determined effective and optimal dose of 1.5 mg siRNA per kg body weight [19]. In addition, a higher dose of 2.5 mg siRNA per kg body weight was injected to mice to investigate possible undesired non-selective silencing of the non-

Table 1
Allele-selective and non-selective siRNAs targeting *Vwf*.

ID	Target		siRNA sequence
si*Control*	–	scrambled si*Vwf*	5′-dTGAUAUUUCCCUcAGUAACgsg-3′
si*Vwf*	**B6**/129S	c.6348-c.6365	5′-dTAUGUUUUCACCaACGUACgsg-3′
si*Control.B6*	–	scrambled si*Vwf.B6*	5′-dTAUAUCCAAUUAcFCCUAAcsa-3′
si*Vwf.B6*	**B6**	c.1010 **T** > C	5′-dTGUACACAAAAUcUUCUCAcsa-3′
si*Control.129S*	–	scrambled si*Vwf.129S*	5′-dTCGACAUCGAACgCGCACAasa-3′
si*Vwf.129S*	129S	c.2739**C** > T	5′-dTAAACAGGGACAcCGCUCCasa-3′

Note: Chemical modifications are indicated as follows: dT = DNA residue; G, C, A, U = RNA residue; g, c, a, u = 2'-O-Methyl modified residue; s = phosphorothioate backbone modification; underlined and bold = position of allele-selective nucleotide specific for B6 strain, not underlined and bold indicates nucleotide target for 129S strain.

targeted *Vwf*-allele.

2.3. Plasma protein and lung mRNA transcript levels

Blood collection and subsequent plasma VWF antigen (VWF:Ag) levels and VWF multimeric pattern, RNA isolation and subsequent lung *Vwf* mRNA transcript levels were measured as described [19]. Additional primers were designed to determine B6-*Vwf* or 129S-*Vwf* allele-selective transcript levels (Table 2).

2.4. Ferric chloride-induced vascular injury of the mesenteric vessels

The effect of siRNA-mediated allele-selective silencing of *Vwf* on thrombosis was studied using the $FeCl_3$-induced vascular injury model as described [24,25]. Briefly, B6 mice were anesthetized with an intraperitoneal (IP) injection with ketamine (100 mg/kg) and xylazine (10 mg/kg), while for B6.129S mice (both males and females) the dose of ketamine was increased to 150 mg/kg. Following anesthesia, circulating blood platelets were fluorescently labeled by a retro-orbital injection with rhodamine 6G dissolved in saline (dose 3.3 mg/kg, Sigma Aldrich). Next, abdomen was opened, mesenteric vessels were exposed, and a 10% $FeCl_3$-immersed (Sigma-Aldrich) filter paper strip was topically placed on the mesenteric vessels. Thrombus development was monitored with an inverted epifluorescent microscope (×10) (Nikon Eclipse TE2000-U) using MetaMorph (v7.8) imaging software for up to 45 min or until occlusion of the vessel. Time to occlusion was the primary outcome parameter, and non-occlusive thrombus development was measured every 5 min for a time period of 45 min in total by an automated quantification pipeline (Supplemental materials) using CellProfiler (version 4.2.1) based on the intravascular rhodamine-positive area [26]. Positive areas smaller than 30 μm in diameter were excluded from measurement, data was presented as the area under the curve of the sum of all thrombi measured over time.

2.5. Tail-bleeding assay

For the tail-bleeding assay, B6.129S mice were anesthetized with an IP injection with ketamine (150 mg/kg), xylazine (10 mg/kg) and atropine (0.1 mg/kg), while B6 and $Vwf^{-/-}$ mice received the ketamine at the dose of 100 mg/kg. The tail was immersed in warm saline (37°C) for 5 min to induce vasodilation and subsequently transected (3 mm) with immediate immersion into a 50 mL tube pre-filled with warm (37°C) saline. Time to cessation of bleeding was recorded and bleeding was considered to have stopped when there was no blood loss visible anymore. If bleeding continued up to the 600-second time point after transection, bleeding was stopped by cauterization of the transection wound and bleeding time was set at 600 s. To determine the volume of blood loss, the tubes with blood and saline were centrifuged at 1500 ×*g* for 20 min RT, the red blood cell pellet was lysed with 20 mL deionized distilled water (ddH_2O) and light absorbance at wavelength of 416 nm was measured. To determine the volume of blood loss (μL), a standard curve was made by pooled whole blood samples of B6 and B6.129S mice.

2.6. Statistical analysis

Graphic illustrations were generated, and statistical analysis was performed using GraphPad Prism 9.3.1 (GraphPad Software, La Jolla, CA, USA). Data is presented as the median with range. Mann-Whitney *U* or Kruskal-Wallis test were used to determine statistically significant differences between two or three experimental groups, respectively. The Fisher's exact test was performed to determine statistically significant differences between the two control groups after occlusive $FeCl_3$-induced thrombosis. $P \leq 0.05$ was considered to be statistically significant.

Table 2
qPCR primer sequences.

Gene	Forward primer	Reverse primer
Gapdh	ACTCCCACTCTTCCACCTTC	CACCACCCTGTTGCTGTAG
Total Vwf	GCCTCAAGCAGAGCACAAAC	TCCTGCAGGCACAGGTAAAG
B6 Vwf	CAGTGAGGAACAGCGGTGTA	CCACAAAGGACTCGGGATCC
129S Vwf	CAGTGAGGAACAGCAGTGCA	CCACAAAGGACTCGGGATCC

3. Results

3.1. Allele-selectivity of siRNAs in B6.129S mice

Administration of the non-selective si*Vwf* (at dose 1.5 mg/kg) in the heterozygous B6.129S mice resulted in a strong significant reduction of median total lung *Vwf* mRNA levels of 81% (Fig. 1A). As expected for this non-selective si*Vwf*, a comparable reducing effect was seen for lung *Vwf* transcript originating from both B6 and 129S alleles (67% and 73%, respectively). In concordance, a strong 87% median reduction of plasma VWF levels was observed for this non-selective si*Vwf*. As anticipated, for the allele-selective si*Vwf.B6*, a limited reduction of 41% of total *Vwf* lung transcript was observed in the heterozygous B6.129S mice (Fig. 1B). For this selective si*Vwf.B6*, reduction of the corresponding *Vwf* transcript from the B6-allele was much stronger than the reduction of lung *Vwf* transcript expressed from the non-corresponding 129S-allele (median reduction in transcript of 66% B6-allele versus 12% 129S-allele). A similar but opposite effect was observed in B6.129S mice that were injected with the allele-selective si*Vwf.129S*. Again, total lung *Vwf* mRNA showed limited reduction by 45% but inhibition of *Vwf* from the 129S-allele was now stronger and >5-fold to that of the non-corresponding B6-allele (median reduction in transcript of 59% 129S-allele versus 9% B6-allele) (Fig. 1C). For both the allele-selective si*Vwf.B6* and si*Vwf.129S* the approximate halving of total lung *Vwf* mRNA coincided with a (corresponding) median reduction of plasma VWF of approximately 50% (Fig. 1B and C, right panels). A higher siRNA dosage of 2.5 mg/kg of si*Vwf.B6* or si*Vwf.129S* in B6.129S mice essentially produced the same results, indicating that upon a higher dosing of the siRNAs, allele-selectivity persisted (Supplemental Fig. 1). The VWF multimeric pattern of 1.5 mg/kg si*Vwf.B6*-treated B6.129S mice was the same compared to si*Control.B6*-treated B6.129S mice (Supplemental Fig. 2), which is to be expected.

si*Vwf.B6* and si*Vwf.129S* were both clearly allele-selective, yielding essentially comparable but opposite effects, and in combination with the previous strong reduction seen by the si*Vwf.B6* in the corresponding homozygous B6 mice [19], we chose to only use the si*Vwf.B6* for experiments focusing on allele-selective inhibition of *Vwf* on experimental thrombosis and bleeding.

3.2. Effect of allele-selective silencing of Vwf on thrombus development

The effect of allele-selective silencing of *Vwf* using si*Vwf.B6* was assessed using the $FeCl_3$-induced vascular injury model, with monitoring of thrombus formation in mesenteric arterioles (Fig. 2, Supplemental Fig. 3) and venules (Supplemental Fig. 4). For B6 mice, after being subjected to $FeCl_3$, 7 out of 8 (88%) si*Control.B6*-treated animals developed occlusive thrombosis, compared to 4 out of 8 si*Vwf.B6*-treated mice (Fig. 2A). Remarkably and unexpectedly, when si*Control.B6*-treated B6.129S mice were subjected to the model, only 3 out of 10 animals developed occlusive thrombi within the 45-minute time (versus 3 out of 20 si*Vwf.B6*-/si*Vwf*-treated B6.129S mice). This poor response in occlusive thrombus formation in B6.129S mice treated with si*Control.B6* ($P = 0.0248$, compared to si*Control.B6*-treated B6 mice with occlusive thrombi), suggests that these B6.129S mice are less responsive to the mesenteric $FeCl_3$ model, at least as executed under the described conditions. It was noticed that despite their young age (3/4 weeks old), all B6.129S mice included, in contrast to B6 mice of the same age, featured considerable presence of adipose tissue surrounding the mesenteric

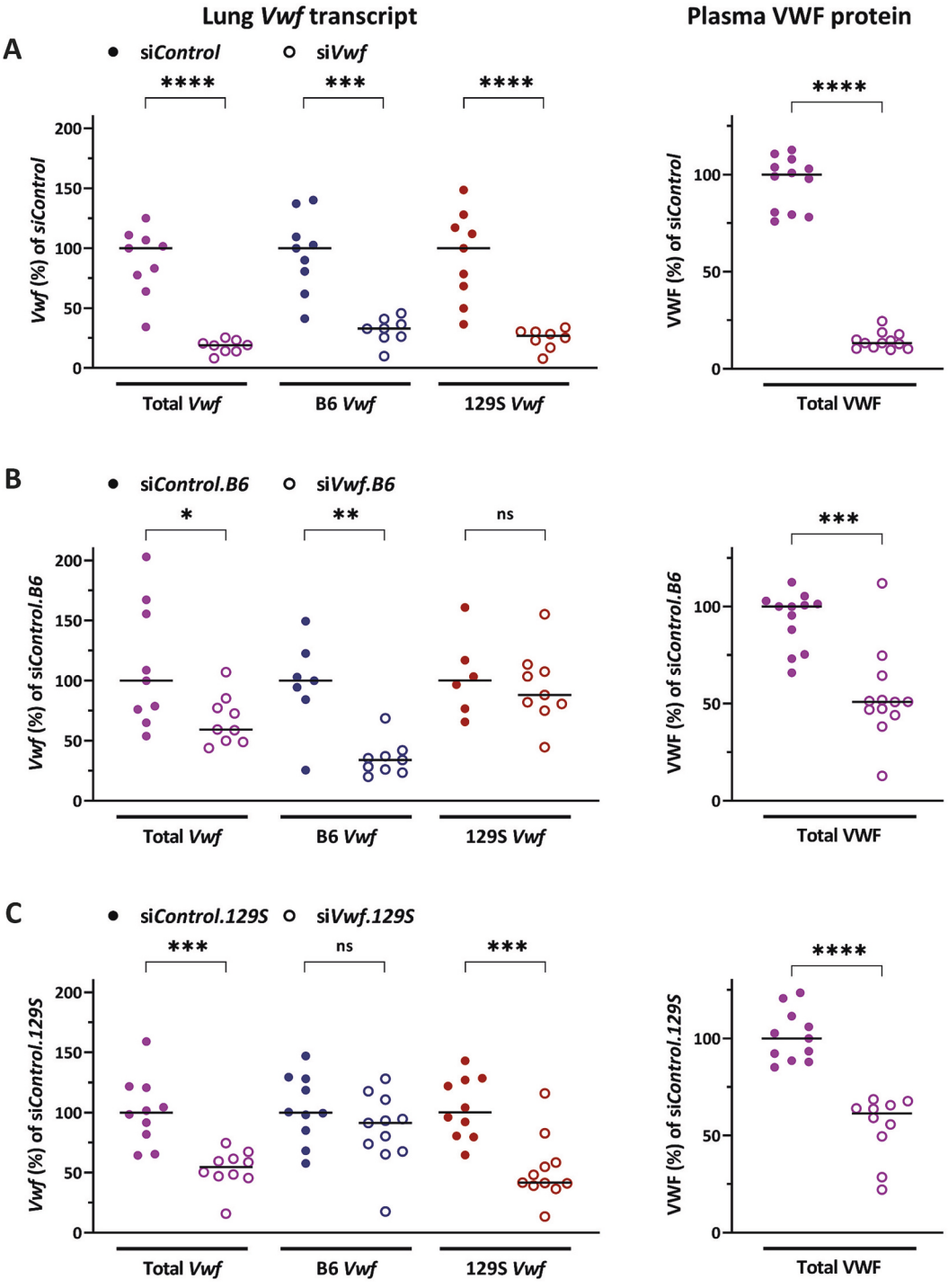

Fig. 1. Effect on VWF expression after siRNA treatment in F1 B6.129S mice. Mice were treated with a non-selective or allele-selective si*Vwf* (open symbols) or with a corresponding scrambled control siRNA (solid symbols) at a dosage of 1.5 mg/kg. A. VWF levels in mice treated with non-selective si*Vwf* or si*Control*. The left graph represents *Vwf* mRNA transcript levels measured in lungs, which were collected 96 h after siRNA injection. Total *Vwf* mRNA is indicated in purple, *Vwf* specific for the B6-allele is indicated in blue and *Vwf* of the 129S-allele in red. Plasma protein levels of the si*Control*- or si*Vwf*-treated B6.129S mice were measured for total VWF (right graph). B. VWF levels measured in si*Vwf.B6*- or si*Control.B6*-treated mice. The left graph represents lung *Vwf* mRNA after si*Vwf.B6* treatment with in purple total *Vwf* mRNA expression levels and in blue (B6) and red (129S) allele-selective *Vwf* transcription levels. Here, the targeted allele was the B6 allele. Plasma VWF levels after siRNA treatment are indicated in the right graph. C. VWF levels measured in si*Vwf.129S*- or si*Control.129S*-treated mice. The left graph represents lung *Vwf* mRNA after si*Vwf.129S* treatment with in purple total *Vwf* mRNA expression levels and in blue (B6) and red (129S) allele-selective *Vwf* transcription levels. Here, the targeted allele was the 129S allele. Plasma VWF levels after siRNA treatment are indicated in the right graph. $N = 12$ animals per treatment group, however, incidentally a data point was excluded because of unwanted clotting activation during blood collection (as established visually), or in the case of the mRNA, due to inconsistent Ct values of the triplicates as result of low quality of the RNA sample. Values of the individual animals are presented with indication of the median value and were compared to the median of the corresponding scrambled control siRNA. Significant differences were determined based on comparisons between groups. $P \geq 0.05$ = ns, $P \leq 0.05$ = *, $P \leq 0.01$ = **, $P \leq 0.001$ = ***, $P \leq 0.0001$ = ****. (For interpretation of the references to color in this figure legend, the reader is referred to the web version of this article.)

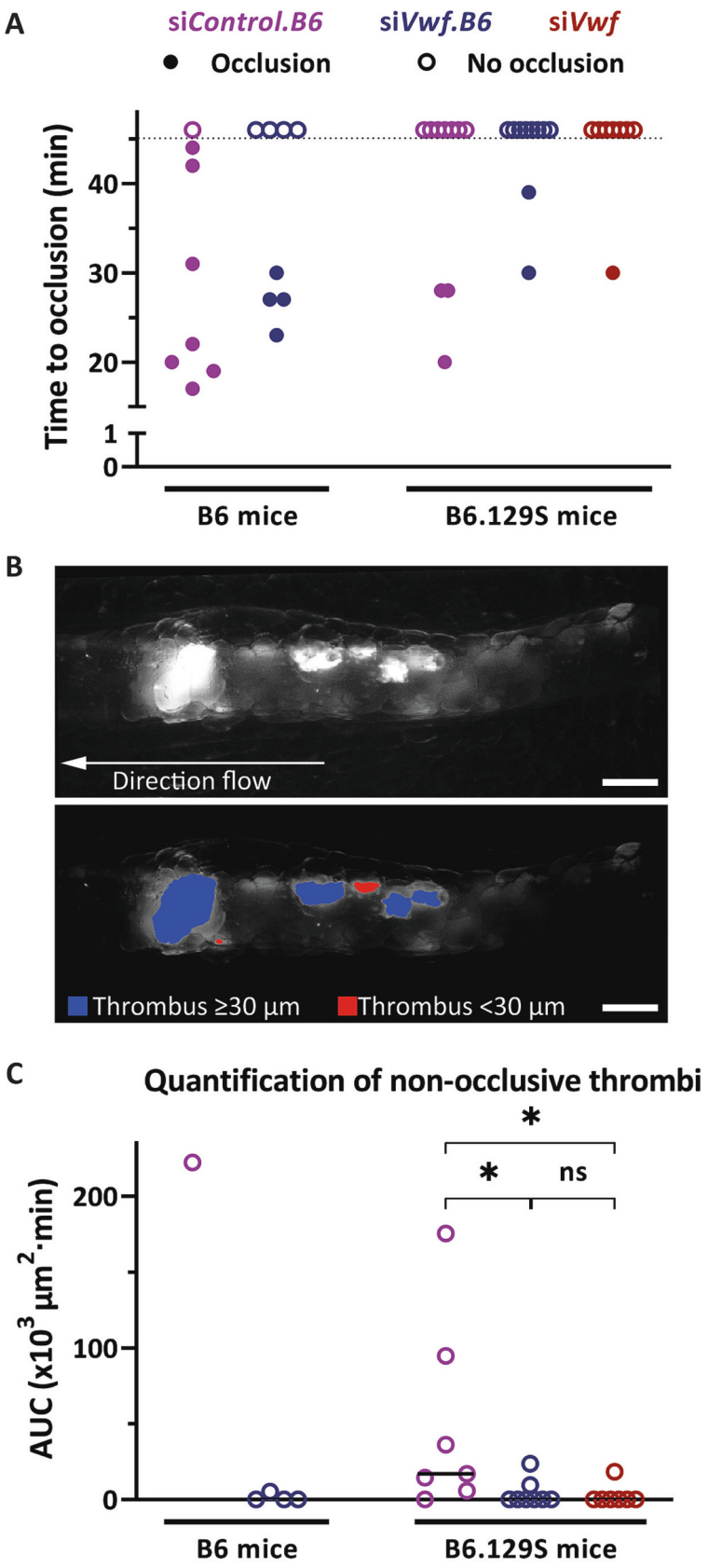

(caption on next page)

Fig. 2. Effect of siRNA treatment on $FeCl_3$-induced thrombosis in arterioles of B6 and B6.129S mice. A. Time to occlusion of arterioles after $FeCl_3$-induced vascular injury in B6 and B6.129S mice treated with si*Control.B6* (purple symbols), si*Vwf.B6* (blue) or si*Vwf* (red). Closed symbols are representative for individual animals that reached occlusion within the 45-minute follow-up period (indicated by dotted line), and open symbols represent animals that did not reach occlusion. Sample sizes per treatment group were as follows: for the B6 mice $N = 8$ si*Control.B6* and si*Vwf.B6*-treated animals; for B6.129S mice N = 8 si*Vwf*-treated animals, $N = 10$ si*Control.B6* and si*Vwf.B6*-treated animals. B. Representative images of CellProfiler output. The upper image is a raw image of an arteriole with thrombus development in white. The lower image shows the processed image with, in blue, thrombi that were included in the measurement as they were over 30 μm in diameter. In red, thrombi that were excluded from measurement (<30 μm diameter) but had high enough intensity to be picked up by the software as a thrombus. Scale bar = 50 μm. C. Thrombus development is indicated as the sum of thrombus surface area measured over a time period of 45 min in si*Control.B6* (purple symbols), si*Vwf.B6* (blue) or si*Vwf* (red) treated mice with non-occlusive arterioles. Values of the individual B6.129S mice are shown with indication of the median value and were compared to the median of si*Control.B6*-treated B6.129S mice. Significant differences were determined based on comparisons between groups. $P \geq 0.05$ = ns, $P \leq 0.05$ = *. (For interpretation of the references to color in this figure legend, the reader is referred to the web version of this article.)

vessels (Supplemental Fig. 5), which may have limited diffusion of $FeCl_3$ into the vessel wall and consequently less or slower induction of vascular injury. Therefore, apart from monitoring occlusive thrombosis, we performed an analysis, focusing on thrombi detectable in the arterioles and venules which did not reach occlusion within the 45-minute time frame (Fig. 2B). In the venules, non-occlusive thrombosis was evident but this was not significantly different between si*Control.B6*- and si*Vwf.B6*-treated B6.129S mice, possibly due to the venules being bigger vessels than the arterioles (Supplemental Fig. 4). In the arterioles, non-occlusive thrombosis was evidently present in si*Control.B6*-treated B6.129S mice and this was significantly reduced in the B6.129S animals treated with si*Vwf.B6* as some of these mice did not develop any thrombi during the 45-minute time period (Fig. 2C). This reduction was comparable to that observed in the non-selective si*Vwf*-treated B6.129S mice. Thus, a thromboprotective effect is observed in B6.129S mice upon reduction of VWF achieved by both a non-selective and allele-selective silencing approach.

3.3. Effect of allele-selective silencing of Vwf on tail-bleeding

First, wild-type (WT) B6 and *Vwf* deficient ($Vwf^{-/-}$; B6 background) mice that did not receive any siRNA treatment were subjected to the tail-bleeding challenge (Fig. 3A). Where the B6 mice stopped bleeding 66.5 [Range 51–124] seconds after tail-tip transection, all $Vwf^{-/-}$ mice continued bleeding up to 600 s of transection and required cauterization of the wound to stop bleeding, which is in concordance with earlier studies [24]. Next, si*Control.B6*-injected B6 mice were challenged and showed a median bleeding time of 54.5 [40–69] seconds comparable to B6 mice without siRNA treatment (Fig. 3A, B). B6 mice that received si*Vwf.B6* showed a heterogenous response, two mice had similar bleeding times to the si*Control.B6* group, two mice did not stop bleeding in the 10-minute observation period, and two mice had a prolonged bleeding time (160 and 186 s) (Fig. 3B). This indicates that the strong reduction in plasma VWF levels by si*Vwf.B6* in B6 mice coincides with an increased bleeding tendency, however this was not as severe as observed for the $Vwf^{-/-}$ mice. Then, B6.129S mice underwent tail-bleeding. When treated with the non-selective si*Vwf*, B6.129S mice showed a small but significant increase in bleeding time in comparison to si*Control.B6*-treated B6.129S mice (82.5 [81–125] vs. 57 [42–68] seconds, Fig. 3B). In contrast, treatment with the allele-selective si*Vwf.B6* did not lead to a significant increase in bleeding time (80.5 [59–118] seconds, Fig. 3B). In addition to bleeding time, the effect on bleeding was also assessed by determining the volume of blood loss. While blood loss results are less outspoken these essentially followed the findings for bleeding times (Supplemental Fig. 6). Thus, allele-selective silencing of *Vwf* does not affect bleeding.

4. Discussion

In this study we have demonstrated, in a complex setting with competing targeted and non-targeted alleles, that allele-selective silencing of *Vwf* in heterozygous B6.129S mice inhibits *Vwf* mRNA of the targeted allele, allowing for a controlled close to 50% reduction of total VWF on plasma level. The hemostatic impact following this 50% reduction of VWF resulted in thromboprotection upon challenging mice with $FeCl_3$-induced vascular injury. Furthermore, this halving of plasma

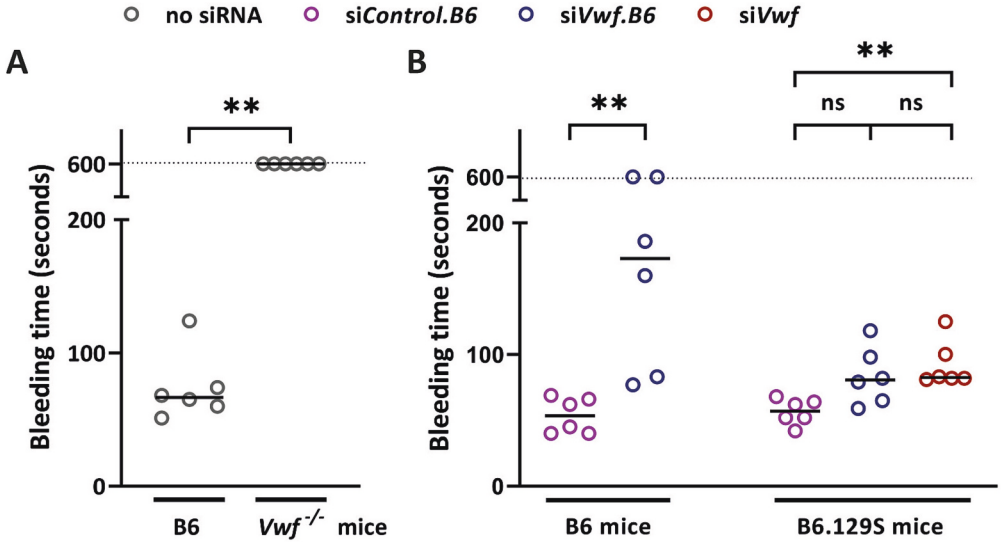

Fig. 3. Effect of siRNA treatment on tail-bleeding in B6 and B6.129S mice. A. Bleeding times in seconds in non siRNA-treated (grey symbols) B6 mice (left) and *Vwf* deficient mice ($Vwf^{-/-}$; right) that underwent tail-bleeding. Tails of mice that did not stop bleeding were cauterized at 600 s (indicated by dotted line). B. Bleeding times in B6 (left) mice and B6.129S mice (right) treated with si*Control.B6* (purple), si*Vwf.B6* (blue) or non-selective si*Vwf* (red). $N = 6$ animals per treatment group; values of individual animals are presented with indication of the median value and significant differences were determined based on comparisons between groups. $P \geq 0.05$ = ns, $P \leq 0.01$ = **. (For interpretation of the references to color in this figure legend, the reader is referred to the web version of this article.)

VWF levels did not lead to prolonged bleeding times.

The mouse strain-selective siRNAs, that we had previously designed against *Vwf* of B6 or 129S mice [19], were now confirmed indeed to be allele-selective in the heterozygous F1 offspring of B6 and 129S crosses. The successful allele-selective silencing of murine *Vwf* follows from targeting just a single nucleotide difference in the *Vwf* gene of B6 and 129S mice and illustrates the major potential of siRNAs in achieving such high levels of selectivity *in vivo*. It should be noted that in the present study only on-target effects, that is the effect on *Vwf* itself, has been assessed. Any possible off-target effects were not investigated in this proof of concept study. In a situation of future clinical application, such off-target effects should be evaluated thoroughly starting with in silico and preclinical studies, now for allele-selective siRNAs developed specifically for the human *VWF* gene. Although the allele-selective siRNAs described in this paper are specific for murine *Vwf* sequences and therefore not applicable to be administered in humans, the method of targeting a single nucleotide difference can act as a proxy for a future human SNP-based targeting approach. Similarly to the allele-selective siRNAs that were used in the current study which were designed based on a single nucleotide difference between the *Vwf* genes of two mouse inbred strains, in a SNP-based targeting approach siRNAs should be designed to target a heterozygous SNP in the human *VWF* gene [27,28]. These heterozygous SNPs preferably have a high minor allele frequency to target larger subpopulations [29]. Application of such an allele-selective siRNA-mediated *VWF*-silencing approach in humans would aim for therapeutic silencing of the allele carrying a dominant-negative *VWF* mutation, present in most type 2 and several type 1 VWD patients [4,5], or just one of the *VWF*-alleles in the context of thrombosis. As mentioned, in the bleeding disorder VWD, hundreds of mutations are known to be linked to the disease [5]. However, designing a therapeutic siRNA for each mutation is not feasible. The SNP-based approach would be a suitable fit for VWD, with allele-selective siRNA-mediated silencing of the mutated *VWF*-allele allowing for an effective and safe reduction of only the diseased VWF. In contrast, in the context of thrombosis, while there are several variants associated with increased plasma VWF levels [30] and increased thrombosis risk [31], currently there are no known mutations in the *VWF* gene to directly cause thrombosis, so here the SNP-based approach would be a suitable option and the allele-selective siRNA-mediated *VWF*-silencing would allow for a safe and thromboprotective 50% VWF reduction.

The impact of a 50% reduction in plasma VWF levels in normal healthy mice was anticipated to be in the window where lowering of VWF coincides with thromboprotection but not bleeding. Studies using mice with one functional *Vwf*-allele ($Vwf^{+/-}$ mice), showed that these mice have similar tail-bleeding-induced bleeding times as compared to mice with 100% VWF functionality [24]. This confirms that a 50% reduction of VWF can be considered safe from a bleeding point of view. In addition, the $Vwf^{+/-}$ mice also benefited from the lower VWF levels when it comes to thrombosis as tested in a $FeCl_3$-induced thrombosis model in the carotid arteries [32]. In $Vwf^{+/-}$ mice, both endothelial and platelet VWF are affected whereas in the siRNA-mediated approach we describe here the platelet VWF remains unaffected [19]. Similar to the earlier studies with $Vwf^{+/-}$ mice, an siRNA-mediated reduction of approximately 50% of plasma VWF in the present study does not lead to prolonged bleeding times and thromboprotection could be achieved even without lowering of platelet VWF. In the context of future therapeutic applications for VWD, this would mean that inhibition of the mutated *VWF*-allele is anticipated to result in a 50 % level of normal plasma VWF activity which will ameliorate the bleeding tendency in VWD patients. In the context of high VWF levels and thromboprotection, a 50% reduction of plasma VWF levels will be a safe approach as it will not lead to an increased bleeding risk.

In the present study, we unexpectedly observed that $FeCl_3$-induced vascular injury led to minimal occlusive thrombus development in normal mice with a B6.129S background (Fig. 3). These findings were less pronounced compared to studies using this well-established model for (arterial) thrombosis, which are predominantly performed on post-weaning 4-/5-week-old mice with a B6 background [24,33–36]. Here, we used 3-/4-week-old B6 and B6.129S mice. One striking difference between these mouse strains, that became evident upon execution of the experiments, was the presence of unexpected excess of adipose tissue surrounding the blood vessels of the B6.129S mice, not the B6 mice. The use of 3-week-old mice in this model was to circumvent presence of adipose tissue as it may have a negative impact on the diffusion of $FeCl_3$ into the mesenteric vessel walls, and subsequent induction of occlusive thrombosis. Although even at the young age of 3 weeks old there was excess adipose tissue, using B6.129S mice younger than 3 weeks to avoid presence of adipose tissue is not possible or desirable from a practical (intravenous siRNA injections, surgery) and ethical point-of-view. While the adipose tissue may have reduced the extent of $FeCl_3$-induced occlusive thrombosis in B6.129S mice, thrombosis formation was still evident, albeit milder and not occlusive. This non-occlusive thrombosis appeared well-measurable and using automated analysis of the non-occlusive thrombus formation over time, allowed detection of thromboprotection upon si*Vwf* or si*Vwf.B6* treatment. This extension of thrombosis analysis within the $FeCl_3$-model can be a valuable addition to the model, and the pipeline for automated analysis developed as part of the present study is freely available (Supplemental materials).

In summary, we have shown allele-selective inhibition of VWF production in heterozygous B6.129S mice with siRNAs designed to specifically target one nucleotide difference between the B6 and the 129S allele. Lowering of VWF led to less thrombosis development, even at a maximum of 50% VWF reduction due to the allele-selective silencing of the *Vwf* gene. Bleeding times were unaffected upon allele-selective si*Vwf* treatment, indicating that 50% less VWF production does not increase the bleeding risk. These results further underline the potential of allele-selective *VWF*-silencing as a customized treatment strategy for hemostatic disorders such as VWD and (arterial) thrombosis.

Authorship

Contributions: YKJ, BJMvV, CVD and JCJE designed the study; ESE and JED prepared and contributed vital reagents; YKJ, NAL and BJMvV performed *in vivo* experiments; YKJ and RJD performed *ex vivo* experiments; YKJ, SNJL, BJMvV, CVD and JCJE analyzed and interpreted the data; YKJ, BJMvV and JCJE wrote the manuscript; all authors have contributed to revisions of the manuscript.

CRediT authorship contribution statement

Yvonne K. Jongejan: Writing – review & editing, Writing – original draft, Visualization, Validation, Software, Methodology, Investigation, Formal analysis, Data curation, Conceptualization. **Noa A. Linthorst:** Writing – review & editing, Data curation. **Elisa Schrader Echeverri:** Writing – review & editing, Conceptualization. **Sebastiaan N.J. Laan:** Writing – review & editing, Software, Formal analysis. **Richard J. Dirven:** Writing – review & editing, Methodology, Data curation. **James E. Dahlman:** Writing – review & editing, Supervision. **Bart J.M. van Vlijmen:** Writing – review & editing, Writing – original draft, Supervision, Methodology, Data curation, Conceptualization. **Cécile V. Denis:** Writing – review & editing, Supervision, Conceptualization. **Jeroen C.J. Eikenboom:** Writing – review & editing, Writing – original draft, Supervision, Project administration, Methodology, Investigation, Funding acquisition.

Declaration of competing interest

The authors declare the following financial interests/personal relationships which may be considered as potential competing interests:

YKJ and JCJE – Dutch Thrombosis Foundation (TSN) grant #2018-01.

NAL and JCJE – Netherlands Organization for Scientific Research

(NWO) NWO-AES grant #18712.

SNJL and JCJE – Netherlands Organization for Scientific Research (NWO) NWA-ORC grant #1160.18.038.

JCJE – CSL Behring research funding.

RJD, ESE, JED, BJMvV, CVD declare they have no known competing financial interests or personal relationships that could have appeared to influence the work reported in this paper.

Acknowledgements

This study was funded by the Dutch Thrombosis Foundation (TSN grant #2018-01).

The contribution of NAL was funded by the Netherlands Organization for Scientific Research (NWO), Domain Applied and Engineering Sciences (TTW), 'Connecting Innovators' Open Technology Programme, Project #18712 and the contribution of SNJL was funded by the Netherlands Organization for Scientific Research (NWO) in the framework of the NWA-ORC Call grant agreement NWA.1160.18.038.

The authors would like to thank Rob F.P. van den Akker, Rayna J.S. Anijs and Ka Lei Cheung for assisting during the animal experiments.

Appendix A. Supplementary data

Supplementary data to this article can be found online at https://doi.org/10.1016/j.thromres.2024.03.002.

References

[1] J.J. Sixma, J. Wester, The hemostatic plug, Semin. Hematol. 14 (3) (1977) 265–299.
[2] A. Gringeri, F.A. Ofosu, S. Grancha, J. Oldenburg, N.P. Ewing, A.B. Federici, Understanding FVIII/VWF complex–report from a symposium of XXIX WFH meeting 2010, Haemophilia 18 (3) (2012) 469–475.
[3] S.W. Pipe, R.R. Montgomery, K.P. Pratt, P.J. Lenting, D. Lillicrap, Life in the shadow of a dominant partner: the FVIII-VWF association and its clinical implications for hemophilia A, Blood 128 (16) (2016) 2007–2016.
[4] F.W. Leebeek, J.C. Eikenboom, Von Willebrand's disease, N. Engl. J. Med. 375 (21) (2016) 2067–2080.
[5] A. de Jong, J. Eikenboom, Von Willebrand disease mutation spectrum and associated mutation mechanisms, Thromb. Res. 159 (2017) 65–75.
[6] M.A. Sonneveld, O.H. Franco, M.A. Ikram, A. Hofman, M. Kavousi, M.P. de Maat, F. W. Leebeek, Von Willebrand factor, ADAMTS13, and the risk of mortality: the Rotterdam study, Arterioscler. Thromb. Vasc. Biol. 36 (12) (2016) 2446–2451.
[7] R.G. Wieberdink, M.C. van Schie, P.J. Koudstaal, A. Hofman, J.C. Witteman, M. P. de Maat, F.W. Leebeek, M.M. Breteler, High von Willebrand factor levels increase the risk of stroke: the Rotterdam study, Stroke 41 (10) (2010) 2151–2156.
[8] P.C.S. van Paridon, M. Panova-Noeva, R. van Oerle, A. Schulz, J.H. Prochaska, N. Arnold, I. Schmidtmann, M. Beutel, N. Pfeiffer, T. Münzel, K.J. Lackner, H. Ten Cate, P.S. Wild, H.M.H. Spronk, Lower levels of vWF are associated with lower risk of cardiovascular disease, Res. Pract. Thromb. Haemost. 6 (7) (2022) e12797.
[9] Y.V. Sanders, J. Eikenboom, E.M. de Wee, J.G. van der Bom, M.H. Cnossen, M. E. Degenaar-Dujardin, K. Fijnvandraat, P.W. Kamphuisen, B.A. Laros-van Gorkom, K. Meijer, E.P. Mauser-Bunschoten, F.W. Leebeek, Reduced prevalence of arterial thrombosis in von Willebrand disease, J. Thromb. Haemost. 11 (5) (2013) 845–854.
[10] S. Sukumar, B. Lämmle, S.R. Cataland, Thrombotic thrombocytopenic purpura: pathophysiology, diagnosis, and management, J. Clin. Med. 10 (3) (2021).
[11] A.C. Weyand, V.H. Flood, Von Willebrand disease: current status of diagnosis and management, Hematol. Oncol. Clin. North Am. 35 (6) (2021) 1085–1101.
[12] N.T. Connell, V.H. Flood, R. Brignardello-Petersen, R. Abdul-Kadir, A. Arapshian, S. Couper, J.M. Grow, P. Kouides, M. Laffan, M. Lavin, F.W.G. Leebeek, S. H. O'Brien, M.C. Ozelo, A. Tosetto, A.C. Weyand, P.D. James, M.A. Kalot, N. Husainat, R.A. Mustafa, ASH ISTH NHF WFH 2021 guidelines on the management of von Willebrand disease, Blood Adv. 5 (1) (2021) 301–325.
[13] M. Subhan, M. Scully, Advances in the management of TTP, Blood Rev. 55 (2022) 100945.
[14] M. Djulbegovic, J. Tong, A. Xu, J. Yang, Y. Chen, A. Cuker, A. Pishko, Adding caplacizumab to standard of care in thrombotic thrombocytopenic purpura: a systematic review and meta-analysis, Blood Adv. 7 (10) (2022) 2132–2142.
[15] F. Conroy, R. Miller, J.F. Alterman, M.R. Hassler, D. Echeverria, B. Godinho, E. G. Knox, E. Sapp, J. Sousa, K. Yamada, F. Mahmood, A. Boudi, K. Kegel-Gleason, M. DiFiglia, N. Aronin, A. Khvorova, E.L. Pfister, Chemical engineering of therapeutic siRNAs for allele-specific gene silencing in Huntington's disease models, Nat. Commun. 13 (1) (2022) 5802.
[16] E.H. Allen, S.D. Atkinson, H. Liao, J.E. Moore, D.M. Leslie Pedrioli, F.J. Smith, W. H. McLean, C.B. Moore, Allele-specific siRNA silencing for the common keratin 12 founder mutation in Meesmann epithelial corneal dystrophy, Invest. Ophthalmol. Vis. Sci. 54 (1) (2013) 494–502.
[17] H. Haybar, E. Khodadi, M. Kavianpour, N. Saki, Mutations and common polymorphisms in ADAMTS13 and vWF genes responsible for increasing risk of thrombosis, Cardiovasc. Hematol. Disord. Drug Targets 18 (3) (2018) 176–181.
[18] J.K. Murray, J. Long, L. Liu, S. Singh, D. Pruitt, M. Ollmann, E. Swearingen, M. Hardy, O. Homann, B. Wu, J.R. Holder, K. Sham, B. Herberich, M.C. Lo, H. Dou, A. Shkumatov, M. Florio, I.C. Rulifson, Identification and optimization of a minor allele-specific siRNA to prevent PNPLA3 I148M-driven nonalcoholic fatty liver disease, Nucleic Acid Ther. 31 (5) (2021) 324–340.
[19] Y.K. Jongejan, E. Schrader Echeverri, R.J. Dirven, K. Paunovska, N.A. Linthorst, A. de Jong, J.C. Wellershoff, K.D. van der Gouw, B.J.M. van Vlijmen, J.E. Dahlman, J.C.J. Eikenboom, Small interfering RNA-mediated allele-selective silencing of von Willebrand factor in vitro and in vivo, Blood Adv. 7 (20) (2023) 6108–6119.
[20] F. Faul, E. Erdfelder, A. Buchner, A.G. Lang, Statistical power analyses using G*Power 3.1: tests for correlation and regression analyses, Behav. Res. Methods 41 (4) (2009) 1149–1160.
[21] R. van Eenige, P.S. Verhave, P.J. Koemans, I. Tiebosch, P.C.N. Rensen, S. Kooijman, RandoMice, a novel, user-friendly randomization tool in animal research, PLoS One 15 (8) (2020) e0237096.
[22] O.F. Khan, P.S. Kowalski, J.C. Doloff, J.K. Tsosie, V. Bakthavatchalu, C.B. Winn, J. Haupt, M. Jamiel, R. Langer, D.G. Anderson, Endothelial siRNA delivery in nonhuman primates using ionizable low-molecular weight polymeric nanoparticles, Sci. Adv. 4 (6) (2018) eaar8409.
[23] J.E. Dahlman, C. Barnes, O. Khan, A. Thiriot, S. Jhunjunwala, T.E. Shaw, Y. Xing, H.B. Sager, G. Sahay, L. Speciner, A. Bader, R.L. Bogorad, H. Yin, T. Racie, Y. Dong, S. Jiang, D. Seedorf, A. Dave, K.S. Sandu, M.J. Webber, T. Novobrantseva, V. M. Ruda, A.K.R. Lytton-Jean, C.G. Levins, B. Kalish, D.K. Mudge, M. Perez, L. Abezgauz, P. Dutta, L. Smith, K. Charisse, M.W. Kieran, K. Fitzgerald, M. Nahrendorf, D. Danino, R.M. Tuder, U.H. von Andrian, A. Akinc, A. Schroeder, D. Panigrahy, V. Kotelianski, R. Langer, D.G. Anderson, In vivo endothelial siRNA delivery using polymeric nanoparticles with low molecular weight, Nat. Nanotechnol. 9 (8) (2014) 648–655.
[24] C. Denis, N. Methia, P.S. Frenette, H. Rayburn, M. Ullman-Culleré, R.O. Hynes, D. D. Wagner, A mouse model of severe von Willebrand disease: defects in hemostasis and thrombosis, Proc. Natl. Acad. Sci. 95 (16) (1998) 9524–9529.
[25] F. Adam, C. Casari, N. Prevost, A. Kauskot, C. Loubiere, P. Legendre, C. Reperant, D. Baruch, J.P. Rosa, M. Bryckaert, P.G. de Groot, O.D. Christophe, P.J. Lenting, C. V. Denis, A genetically-engineered von Willebrand disease type 2B mouse model displays defects in hemostasis and inflammation, Sci. Rep. 6 (2016) 26306.
[26] D.R. Stirling, M.J. Swain-Bowden, A.M. Lucas, A.E. Carpenter, B.A. Cimini, A. Goodman, CellProfiler 4: improvements in speed, utility and usability, BMC Bioinformatics 22 (1) (2021) 433.
[27] A. De Jong, R.J. Dirven, J.A. Oud, D. Tio, B.J.M. Van Vlijmen, J. Eikenboom, Correction of a dominant-negative von Willebrand factor multimerization defect by small interfering RNA-mediated allele-specific inhibition of mutant von Willebrand factor, J. Thromb. Haemost. 16 (7) (2018) 1357–1368.
[28] A. de Jong, R.J. Dirven, J. Boender, F. Atiq, S.Y. Anvar, F.W.G. Leebeek, B.J.M. van Vlijmen, J. Eikenboom, Ex vivo improvement of a von Willebrand disease type 2A phenotype using an allele-specific small-interfering RNA, Thromb. Haemost. 120 (11) (2020) 1569–1579.
[29] A. Auton, L.D. Brooks, R.M. Durbin, E.P. Garrison, H.M. Kang, J.O. Korbel, J. L. Marchini, S. McCarthy, G.A. McVean, G.R. Abecasis, A global reference for human genetic variation, Nature 526 (7571) (2015) 68–74.
[30] A.H. Mufti, K. Ogiwara, L.L. Swystun, J.C.J. Eikenboom, U. Budde, W.M. Hopman, C. Halldén, J. Goudemand, I.R. Peake, A.C. Goodeve, D. Lillicrap, D.J. Hampshire, The common VWF single nucleotide variants c.2365A>G and c.2385T>C modify VWF biosynthesis and clearance, Blood Adv. 2 (13) (2018) 1585–1594.
[31] R. Schneppenheim, N. Hellermann, M.A. Brehm, U. Klemm, T. Obser, V. Huck, S. W. Schneider, C.V. Denis, A. Tischer, M. Auton, W. März, E.R. Xu, M. Wilmanns, R. B. Zotz, The von Willebrand factor Tyr2561 allele is a gain-of-function variant and a risk factor for early myocardial infarction, Blood 133 (4) (2019) 356–365.
[32] S. Jäckel, K. Kiouptsi, M. Lillich, T. Hendrikx, A. Khandagale, B. Kollar, N. Hörmann, C. Reiss, S. Subramaniam, E. Wilms, K. Ebner, M.V. Brühl, P. Rausch, J.F. Baines, S. Haberichter, B. Lämmle, C.J. Binder, K. Jurk, Z.M. Ruggeri, S. Massberg, U. Walter, W. Ruf, C. Reinhardt, Gut microbiota regulate hepatic von Willebrand factor synthesis and arterial thrombus formation via toll-like receptor-2, Blood 130 (4) (2017) 542–553.
[33] M. Rybaltowski, Y. Suzuki, H. Mogami, I. Chlebinska, T. Brzoska, A. Tanaka, F. Banno, T. Miyata, T. Urano, In vivo imaging analysis of the interaction between unusually large von Willebrand factor multimers and platelets on the surface of vascular wall, Pflugers Arch. 461 (6) (2011) 623–633.
[34] A.M. Navarrete, C. Casari, P. Legendre, I. Marx, J.R. Hu, P.J. Lenting, O. D. Christophe, C.V. Denis, A murine model to characterize the antithrombotic effect of molecules targeting human von Willebrand factor, Blood 120 (13) (2012) 2723–2732.
[35] A. Reheman, P. Gross, H. Yang, P. Chen, D. Allen, V. Leytin, J. Freedman, H. Ni, Vitronectin stabilizes thrombi and vessel occlusion but plays a dual role in platelet aggregation, J. Thromb. Haemost. 3 (5) (2005) 875–883.
[36] W. Li, M. Nieman, A. Sen Gupta, Ferric chloride-induced murine thrombosis models, J. Vis. Exp. 115 (2016).